Title:

NF-κB links CO_2 sensing to innate immunity and inflammation in mammalian cells.

Running Title:

NF-κB, CO_2 sensing, innate immunity and inflammation

Eoin P. Cummins, Kathryn M. Oliver, Colin R. Lenihan, Susan F. Fitzpatrick, Ulrike Bruning, Carsten Scholz, Craig Slattery, Martin O. Leonard, Paul McLoughlin and Cormac T. Taylor.

UCD Conway Institute for Biomolecular and Biomedical research, University College Dublin, Belfield, Dublin 4, Ireland.

This work was supported by a grant from the Science Foundation of Ireland and the Health Research Board.

Address correspondence: Eoin P. Cummins PhD,

Telephone: (00353)-87-3536132

email: eoin.cummins@ucd.ie

Fax: (00353)-1-7166701

Character count: ~56,395

Abstract:

Molecular oxygen (O_2) and Carbon dioxide (CO_2) are the primary substrate and product of aerobic metabolism respectively. Levels of these physiologic gases in the cell microenvironment vary dramatically both in health and in diseases such as chronic inflammation, ischemia and cancer where significant changes in metabolism occur. The identification of the hypoxia-inducible factor (HIF) led to the discovery of an ancient and direct link between tissue O_2 and gene transcription. Here, we demonstrate that mammalian cells (Mouse embryonic fibroblasts (MEF) and others) also sense changes in local CO_2 levels leading to altered gene expression via the NF-κB pathway. IKKα, a central regulatory component of NF-κB, rapidly and reversibly translocates to the nucleus in response to elevated CO_2. This response is independent of HIF, extracellular and intracellular pH or pathways which mediate acute CO_2-sensing in nematodes and flies and leads to attenuation of bacterial lipopolysaccharide-induced gene expression. These results suggest the existence of a molecular CO_2 sensor in mammalian cells which is linked to the regulation of genes involved in innate immunity and inflammation.

Keywords: Carbon dioxide/ hypercapnia/ inflammation/ immunity/ NFκB.

Introduction:

Changes in intracellular O_2 are sensed by a family of proline and asparagine hydroxylases leading to altered gene transcription via the Hypoxia Inducible Factor (HIF) which governs the adaptive response to hypoxia (1, 2). In earlier work, we demonstrated that NF-κB, a master regulator of innate immune and inflammatory gene expression is induced by hypoxia through a similar hydroxylase-dependent mechanism (3).

CO_2 production is coupled to oxygen consumption. As a result, physiologic CO_2 levels are higher in tissues than in the atmosphere and can change dramatically under conditions where cellular metabolism is altered. Acute CO_2-sensing has been reported in specialised cells in several lower animal species including flies, nematodes and rodents leading to rapid neuronal signaling which directs responses as diverse as survival, avoidance and olfactory sensation (4-6). However, little is known regarding the impact of altered CO_2 on gene expression.

Permissive hypercapnia which occurs when blood pCO_2 is elevated during hypoventilation of intubated patients, attenuates mortality during acute respiratory distress syndrome (ARDS) (7). Similarly, hypercapnic-acidosis attenuates endotoxin-induced acute lung injury supporting a generally anti-inflammatory effect of CO_2 (8). Furthermore, elevated CO_2 increases mortality in *Drosophila* exposed to pathogens and augments infection-induced injury in rats indicating a role for CO_2-sensing in suppression of innate immunity (9, 10). NF-κB, is a key transcriptional regulator of inflammation and innate immunity (11).

Recent studies have implicated altered NF-κB signaling in the attenuation of inflammatory gene expression by hypercapnic-acidosis and in the regulation of the Drosophila NF-κB homologue Relish by CO_2 (9, 12). In this paper we describe a novel CO_2- dependent nuclear localisation of the NF-κB signaling protein IKKα. The sensitivity of IKKα to CO_2 is rapid, reversible and dose dependent. It is independent of the hypoxia signaling pathway, pathways involved in CO_2 sensing in lower species, extracellular and intracellular pH. The CO_2 –dependent nuclear localisation of IKKα is associated with a marked attenuation of NF-κB signaling with effects evident at the level of cytoplasmic IκBα, nuclear p65, and NF-κB target gene expression.

Materials and Methods:

Cell Culture

MEF, HK-2, Hela, CCD-19Lu, A549 and primary human peripheral blood mononuclear cells (PBMCs) were cultured at 21% O_2, 5% CO_2 and maintained in a humidified tissue culture incubator prior to exposure to the conditions indicated in the individual experiments. Media used in each case was specific to each cell type. All reagents produced by Gibco unless indicated otherwise. MEF media: DMEM high glucose with L-glutamine supplemented with 10% FCS, Penicillin/ Streptomycin (P/S); Hela and CCD-19Lu media: MEME, 10% FCS, P/S, L-glutamine, Non-essential amino acids (Sigma), HK-2 media: (DMEM / Hams F12 (1:1) (Sigma) P/S, L-glutamine, 10ng/ml EGF + supple

PBMC Media: Medium 199/EBSS + Earles balanced salts + L-glutamine (Thermo), P/S, 10% Human serum, Polymixin B Sulfate 10μg/ml.

PBMC isolation and culture

Whole blood was drawn from human volunteers and immediately added to a BD Vacutainer CPT cell preparation tube with sodium citrate. Blood was centrifuged within 30 mins of drawing and centrifuged at 1500 rcf for 20 mins. Mononuclear fraction of cells was isolated and washed x 2 with 10-15mls PBS with centrifugation at 300 rcf for 15mins in between. Cells were then re-suspended in appropriate media in flasks. Media was changed on day 4 and 8. Experiment was carried out on day 9.

Media types used in the experiments

Hypoxia experiments: Cell specific media as indicated above was used for each cell type for the hypoxia/ graded oxygen experiments **(Figures 1A, 1B and Supplementary Figures 1A, 1B (S1A, S1B)).**

Hypercapnia experiments: MEF media diluted (9:1) with 100mM HEPES (pH 6.8) (Sigma) was used for the initial hypercapnia experiments **(Figures 1C, 2-4 and Supplementary Figure 1C).**

Buffered hypercapnia experiments: MEF media diluted (9:1) with 250mM HEPES (pH 7.3) and supplemented with concentrated HCl or NaCl (to correct for osmolarity change) and equilibrated overnight at 0% or 10% CO_2 prior to experimentation **(Figures 1D-E, 5, 7 and Supplementary Figure 3, 5, 6, 7.**

Graded pH experiments: DMEM high glucose powder supplemented with HEPES (Sigma # D2903 (Figure 6) & Sigma # D1152 (supplementary figure 4)) was re-constituted, filter-sterilised and supplemented with FCS (10%) and P/S. A range of $NaHCO_3$ (Sigma) concentrations were prepared in the media for the distinct media compositions (a range of NaCl (Sigma) concentrations were supplemented to correct for osmolarity differences between the media types). Media was equilibrated for 4 hours at 0.03% or 10% CO_2 prior to experimentation. **(Figure 6 and Supplementary figure 4).**

Preparation of cytosolic and nuclear fractions

Cells were grown for the indicated time period in normoxia/hypoxia/hypercapnia in an open environment (I) or closed chamber (C). In the case of cells from (C) extracts were prepared in the closed chamber. The media was aspirated and cells placed on ice. Cells were then washed briefly in ice cold PBS. The PBS was then aspirated, and 200μl of cytosolic-extract lysis buffer - Buffer A (10mM Hepes (pH8), 1.5mM $MgCl_2$, 10mM KCl, 200mM sucrose, 0.5mM DTT, 0.25% NP-40 (IPEGAL)+ protease inhibitor cocktail) was added to the Petri dish (100mm). Cells were left to swell for 5-10 mins on ice before being scraped with a rubber policeman. Lysate was then centrifuged at 12,000 rpm for 1 min at 4 ^{o}C. The supernatant is the cytosolic fraction. Cytosolic extract was stored at -20 ^{o}C.

The pellet was then washed with 500μl of Buffer A and centrifuged again at 12,000 rpm for 1 min at 4 ^{o}C. The supernatant was discarded and the pellet was re-suspended in 100μl of nuclear-extract lysis buffer, Buffer C (20mM Hepes (pH8), 420mM NaCl, 0.2mM EDTA, 1.5mM $MgCl_2$, 0.5mM DTT, 25% glycerol + protease inhibitor cocktail), and rocked on ice for 30 min. The 1.5ml eppendorf tube was briefly vortexed before centrifuging at 14,000 rpm for 10 min at 4 ^{o}C. The supernatant contains the nuclear fraction. Nuclear fraction was stored at -80 ^{o}C. Fractionation was validated by enrichment of a predominantly cytosolic protein IκBα in the cytosolic fraction and enrichment of a nuclear protein Lamin A/C in the nuclear fraction (as well as enrichment of p65 in the nuclear fraction

following ligand activation)

Immunoblotting. Western blotting of cytosolic and nuclear fractions was carried out according to standard protocols using the following primary antibodies IKKα (#2682), IKKβ (#2370) Lamin A/C (#2032), IκBα (#4814), (all Cell Signalling), p65 (#sc-372) (Santa Cruz), β-actin (Sigma), HIF-1α (H1a67) (Calbiochem), Tata box binding protein (abcam).

Transient Transfection. Transient transfection of plasmid DNA was performed in subconfluent cells using Lipofectamine 2000 (Invitrogen) transfection reagent according to the manufacturer's instructions. After transfection, cells were exposed overnight at 37°C (21% O_2, 5% CO_2). 24hrs later media was replaced and cells were exposed to experimental treatment as described.

Reporter Assay. Cells were transfected with an NF-kappaB-luciferase promoter-reporter construct (Promega # E849A). Cell lysates were prepared by using a 1x luciferase lysis buffer (Promega). Substrate was added to the cell lysate and luciferase activity was measured using a desk-top luminometer (Berthold technologies). Experiments were carried out in duplicate and luciferase values were normalized to co-transfected β-Gal control vector activity.

Fluorescent Microscopy

Cell Fixation and immunostaining. MEF cells were grown on glass coverslips and exposed .03% or 10% CO_2 for the indicated times. The cells were then washed twice with PBS and fixed with 3% Paraformaldehyde (solutions were pre-equilibrated to the respective CO_2 environment). This was followed by further washes with PBS and the quenching of free aldehyde groups with 50mM Ammonium Chloride/PBS. The cells were washed with PBS as before and permeabilised with 0.1% Triton 100. Two more PBS washes followed this before the cells were incubated in primary antibody diluted in 5% FCS/PBS (IKK〈 1:50 Santa Cruz) in a closed humid chamber for 1 hour. Following this cells were washed with PBS as before and incubated with secondary antibody (Alexa Fluor 568 goat ant-rabbit IgG 1:100 Invitrogen) diluted in 5% FCS/PBS in a closed humid chamber for 1 hour. The fixed cells were then washed as before and rinsed in distilled water before inversion and mounting on a glass slide (Dakocytomation fluorescent mounting medium (DakoCytomation)). The slides were then protected from light overnight before imaging.

Confocal Imaging. Confocal imaging was performed using a Carl Zeiss LSM510 UVMETA system mounted on an Axiovert 200M computer controlled microscope. Alexa Fluor 568 was excited using a 543nm laser line from a helium-neon laser and the images were acquired with a 63X Plan-Apo oil immersion objective.

Real-time PCR

RNA Extraction. Total RNA was prepared from cell using Trizol (Qiagen) and isopropanol precipitation or RNeasy spin columns (Qiagen) according to the manufacturer's instructions. First strand cDNA synthesis was performed using random primers and Superscript II reverse transcriptase according to the manufacturer's instructions (Invitrogen).

Quantitiative Real Time PCR

Real Time PCR was performed on an Applied Biosystems 7900HT fast real-time PCR system using mouse primers (Eurofins MWG Operon) or human primers (SABiosciences). The values obtained were normalised to 18S or β-actin and calculated according to the ΔCT method.

PCR array

A549 cells were exposed to ambient or 10% CO_2 for 4hrs +/- Lymphotoxin α1/β2 (100ng/ml). cDNA was generated from RNA and incubated on a "NF-κB Signalling Pathway" RT^2 qPCR array (SABiosciences) according to the manufacturer's instructions. This array contains 84 key genes involved in the NF-κB signal transduction pathway and several controls. Target genes were normalized to control β-actin expression and expressed as fold change relative to ambient CO_2 control.

Intracellular pH BCECF assay

MEF were washed in serum free media and loaded with 5μM BCECF-AM (Molecular Probes) in Optimem1 (Gibco) for 30 mins at 37^{o}C, 21% O_2, 5% CO_2. Dye was removed and cells were incubated in full DMEM media for 30 mins at 37^{o}C, 21% O_2, 5% CO_2. Cells were then exposed to pre-equilibrated neutral or acidic media at 0.03% CO_2 or 10% CO_2 for 1hr. Following exposure cells were immediately assayed in a fluorescent plate-reader at RT at 21% O_2, ambient CO_2. The fluorophore was excited at 485nm (λ1) and 444nm (λ2) and emission was recorded at 538nm in each case. The ratio λ1:λ2 is directly proportional to intracellular pH.

Tryptan Blue cell viability assay.

A549 cells were exposed to ambient or 10% CO_2 for 4hrs. Culture media was collected and cells were washed once with PBS. PBS was collected and cells were trypsinised using 10x Trypsin. Trypsinisation was blocked using full media and cells were collected with a pipette. Cells were centrifuged at 4^{o}C for 5mins at 1000rpm. Pelleted cells were re-suspended in full medium. 10μl of the re-suspended cells was combined with 10μl Tryptan Blue solution. Viable and no-non viable cells were counted on a haemocytometer and scored in duplicate for n=3 experiments.

Results:

We investigated the impact of altered atmospheric oxygen (1% - 21%) and carbon dioxide (0.03 - 5%) on NF-κB signaling in mammalian cells (Figure 1A). Mouse embryonic fibroblasts (MEF) were treated with DMOG (a pan-hydroxylase inhibitor) or an atmosphere of 1%O_2/5%CO_2 without (H) or with (R) re-equilibration to ambient conditions (21%O_2/ 0.03%CO_2). While nuclear HIF accumulation was detected with DMOG treatment or exposure to 1%O_2/ 5%CO_2, nuclear IKKα accumulation was detected only in cells exposed to 1%O_2/ 5%CO_2 (Figure 1A) indicating that nuclear-translocation of IKKα is independent of hydroxylase-dependent oxygen sensing. This response occurred in multiple cell lines and was rapid and reversible with re-equilibration of cells to ambient conditions (Figures 1A, S1A and S1B).

In order to determine the relative contribution of O_2 and CO_2 to this response, we examined IKKα nuclear translocation in MEF exposed to increasing atmospheric oxygen concentrations against a background of 5% CO_2, without (H) and with (R) re-equilibration to ambient conditions. Reversible nuclear IKKα accumulation occurred in cells exposed to atmospheric oxygen concentrations up to 21% (with 5% CO_2) leading us to hypothesize that the nuclear localization of IKKα is independent of changing O_2 levels but dependent upon exposure to elevated CO_2 (Figures 1B and S1C).

To test this, MEF were exposed to increasing CO_2 levels (0.03-10% with a balance of room air) and cells were either allowed to re-equilibrate to ambient CO_2 (R) or retained at the indicated CO_2 concentration at which nuclear lysates

were prepared (H). Cells re-equilibrated to ambient CO_2 demonstrated loss of nuclear IKKα accumulation thus confirming the existence of a rapidly reversible, CO_2-dependent nuclear localization of IKKα (Figure 1C). This response is evident over a range of physiologic CO_2 concentrations (Figure S1D). Con-focal microscopic analysis of cells exposed to 10% CO_2 with and without re-equilibration to ambient CO_2 confirmed reversible, CO_2-dependent nuclear localization of IKKα (Figure 1D). Our observations were further supported by a robust CO_2 –dependent nuclear localisation of IKKα in primary human PBMCs exposed to 10% CO_2 (Figure 1E).

A number of regulatory roles for nuclear IKKα have been described (13-16). We investigated the effects of elevated CO_2 on activation of the canonical NF-κB signaling pathway in response to activation by LPS. 10% CO_2 inhibited LPS-induced nuclear translocation of the p65 subunit of NF-κB which was co-incident with nuclear translocation of IKKα (Figure 2A). Furthermore, in wild type MEF, 10% CO_2 suppressed LPS-induced NF-κB activity as determined by a luciferase reporter assay (Figure 2B).

IKKα is an active component of the IKKα/β/γ signalling complex but can also exist as a homodimer which can contribute to non-canonical NF-κB signalling (11). We investigated whether the IKKα response to CO_2 is dependent upon its association with IKKβ. IKKα/β double knockout MEF (17) were reconstituted with catalytically active IKKα (18). IKKα –reconstitution in these cells confers sensitivity of the NF-κB-Luc construct to LPS (Figure S2). In IKKα reconstituted

cells, 10% CO_2 significantly attenuated LPS-induced NF-κB activity (Figure 3A). Furthermore, in IKKα–reconstituted MEF there is a robust nuclear localisation of IKKα protein in response to CO_2 (Figure 3B). These data demonstrate that in MEF the IKKα nuclear localisation and inhibition of NF-κB activity is independent of its association with IKKβ.

The signalling consequences of changes in atmospheric CO_2 have been best characterised in flies and nematodes. In *Drosophila*, CO_2 is detected by a mechanism involving Gr21a and Gr63 chemosensory receptors that transduce this input into the physiological response of CO_2 avoidance (4). The guanyl cyclase pathway has also been demonstrated to be important in CO_2 avoidance as demonstrated in nematodes that have mutations in Tax-2 and Tax-4 cGMP gated channels (5). In rodents, olfactory sensory neurons detect CO_2 via carbonic anhydrase mediated-catalysis of CO_2 into bicarbonate which in turn signals through guanyl cyclase D (6) Interestingly, the role of carbonic anhydrase in acute CO_2 sensing is also evident in plants (19, 20). Pseudohyphal development in response to CO_2 in C. albicans is absent in mutants lacking adenylyl cyclase which is thought to act downstream of carbonic anhydrase following detection of CO_2/bicarbonate (21). Taken together there is evidence from lower species that acute CO_2 sensing is mediated through chemosensory neurons in part via carbonic anhydrase, guanylyl cyclase and / or adenylyl cyclase (summarised in the schematic Figure 4A). We investigated whether similar pathways contribute to the IKKα-dependent modulation of the NF-κB pathway by CO_2 in mammalian cells. MEF pre-treated with inhibitors of carbonic

anhydrase (Acetazolamide, 10-500μM) or guanylyl cyclase (ODQ, 100 μM) or an adenylyl cyclase agonist (Forskolin, 10μM) was without significant effect on the CO_2-induced nuclear accumulation of IKKα (Figure 4 B). This data suggests the existence of an intracellular CO_2 sensor pathway linked to IKKα nuclear translocation and suppression of NF-κB which is independent of pathways which mediate acute CO_2 sensing in lower species.

Changes in CO_2 are inextricably linked to changes in intra- and extra-cellular pH. We next investigated whether changes in extracellular pH contribute to CO_2-induced IKKα nuclear localisation. Culture media for use at ambient (0.03%) CO_2 was adjusted with concentrated HCl and equilibrated overnight to pH-match it with osmolarity-corrected culture media for use at 10% CO_2. Under these conditions of tightly buffered extracellular pH (Figure 5A), MEF were exposed to 0.03% or 10% CO_2 for 4hrs +/- LPS (10μg/ml) for the final hour. Despite the buffered pH, IKKα accumulated in the nuclear fraction following exposure to 10% CO_2. Suppression of LPS-induced p65 nuclear accumulation and cytoplasmic IκBα degradation in hypercapnia was also observed (Figure 5B and 5C). This effect is also evident at more moderate (5%) CO_2 levels (Supplementary Figure 3) Our findings are consistent with recent studies in Drosophila that provide evidence for hypercapnia-mediated immunosuppression which is independent of acidosis (9).

Similarly, exposure of MEF to medium designed to have either neutral (N) or acidic (A) pH values (achieved through the addition of sodium bicarbonate and osmolarity balanced using equiosmolar NaCl (Figure 6A-D)), had no effect on the

nuclear localisation of IKKα at ambient CO_2 levels while 10% CO_2-induced IKKα nuclear localisation was no different between neutral or acidic media (Figure 6A and 6B). (The insensitivity of IKKα to extracellular pH change is further demonstrated over a wider range of pH values (Supplemental Figure 4)). Furthermore, there was no significant difference in intracellular pH detected in MEF exposed to these conditions that can account for the nuclear localisation of IKKα at 10% CO_2 (Figure 6D). Based on these data, we hypothesize that elevated CO_2 affects NF-κB signalling in a manner which is independent of changes in extracellular or intracellular pH.

Finally, to investigate the impact of this response in terms of altered gene expression, we investigated the impact of elevated CO_2 on NF-κB-dependent gene expression. To do this we exposed A549 cells to ambient or 10% CO_2 for 4hrs +/- the NF-κB ligand Lymphotoxinα1β2 (LT, 100ng/ml) (using buffered media). (Cell viability was not affected under these conditions (Supplementary Figure 7)). cDNA generated from these cells was assayed on a PCR array with 84 genes with known associations to the NF-κB signaling pathway. A number of genes differentially regulated at 10% CO_2 were selected for validation. These include the chemokine CCL2 (MCP-1), the adhesion molecule ICAM-1, the pro-inflammatory cytokine TNFα, and the anti-inflammatory cytokine IL-10 (Figure 7A-D). (The full array data is included as Supplementary Table 1 and includes evidence for a global effect of CO_2 on the NF-κB transcriptional response. Other genes of interest that were differentially regulated in the array include Toll like

receptor (TLR) family members and other inflammatory mediators such as IL-6 which has recently been described to be affected by elevated CO_2 in macrophages (22).) Interestingly, the expression of the genes associated with a pro-inflammatory response (CCL2, ICAM-1 and TNFα) were blunted at 10% CO_2 while expression of IL-10 which is known to have anti-inflammatory properties (23) was enhanced at 10% CO_2 in the presence of LT (Figure 7 A-D). Furthermore, using two different ligands in a different cell line (MEF) we observe that LPS- and TNFα-induced induction of CCL2 was significantly blunted at 10% CO_2 when compared to ambient CO_2 under pH buffered conditions (Supplementary Figure 5). Taken together these data are strongly supportive of CO_2 -mediated transcriptional changes that result in an anti-inflammatory/immunosuppressive phenotype.

The contribution of IKKα to the suppression of NF-κB signalling at 10% CO_2 was next investigated using an siRNA based approach. A549 cells with and without IKKα siRNA treatment were exposed to ambient or 10% CO_2 with and without LT or TNFα. Hypercapnia clearly affects the cytoplasmic expression of inhibitory protein IκBα in the presence and absence of a ligand in cells treated with non-target siRNA. Interestingly, the effect of 10% CO_2 on IκBα is still evident in cells treated with IKKα siRNA (Supplementary Figure 6). Thus, it appears that while the cellular localisation of IKKα is profoundly influenced by CO_2, it may not be directly responsible for the suppressive effects on NF-κB signalling observed further downstream. An important caveat, however, is that IKKα has a role as a positive regulator of NF-κB signalling as part of the IKK complex and also as part

of the non-canonical signalling pathway. Furthermore, the knockdown of IKKα by siRNA while significant is not a complete knockdown. This may allow for residual IKKα to translocate to the nucleus at 10% CO_2 and elicit suppressive effects on NF-κB target genes which have been described previously (13, 15),(16). On the balance of evidence it appears that there are at least two inputs for CO_2 sensitivity within the NF-κB pathway. The first is the profound rapid, reversible, dose-dependent nuclear localisation of IKKα that occurs in response to elevated CO_2 (1-10%). The second is at the level of IκBα where cytoplasmic expression of this inhibitory protein are maintained/ enhanced against a background of elevated CO_2 (5-10%) which likely attenuates downstream NF-κB target gene expression.

Discussion:

CO_2 has traditionally been considered a waste product of respiration and its biological activity (in terms of gene expression) poorly understood. However, a recent study reported differential gene expression in elevated CO_2 (9). Furthermore, CO_2 has been implicated in development, motility and lifespan in *C. elegans* (24).

Canonical NF-κB signalling is characterised by activation of the IKKα/β/γ "signalsome" by upstream adaptor molecules in response to a ligand. IKKα has a nuclear localisation sequence (NLS) in the N-terminal domain (14) and nuclear IKKα may act as a counter balance to the pro-inflammatory signalling of IKKβ (25). Furthermore, nuclear IKKα may mediate cytokine-induced Histone H3 phosphorylation at specific promoters, thus modifying histone function and inflammatory gene expression (13, 15),(16).

In the current study we provide evidence for rapid, reversible IKKα nuclear localisation in a CO_2-dependent manner over a range of physiological CO_2 concentrations which is associated with an attenuation of LPS-induced NF-κB signalling and target-gene expression consistent with CO_2 affecting IKKα and

contributing to the attenuation of inflammation. Whether IKKα is directly modified by CO_2 or whether the CO_2-sensitivity is conferred by an upstream signalling / adaptor protein has yet to be determined. Furthermore, it appears that the NF-κB pathway may be modified at more than one point by CO_2 as evidenced by the preservation of cytoplasmic IκBα in response to ligand stimulation at elevated CO_2 (5-10%). This is consistent with observations made in hypercapnic acidosis by Takeshita et al. (12) but different from a recent paper from Wang et al. using hypercapnia (22). What is clear is the profound immune and inflammatory signalling consequences for NF-κB target gene expression against a background of elevated CO_2 (10%). Our observations are consistent with those made by both Takeshita et al. (12) and Wang et al. (22). In mammalian models, beneficial immunomodulatory effects of CO_2 have been demonstrated in acute respiratory distress syndrome (ARDS), hypercapnic acidosis and sepsis (7, 8),(26). In *Drosophila*, increased susceptibility to bacterial infection at elevated CO_2 is independent of pH change (9). Furthermore, increased susceptibility to infection persists in rats with normal renal buffering of hypercapnic-acidosis (27) which in the absence of acidosis is suggestive of pH- independent, CO_2 –dependent immunosuppression. Our current work suggests the existence of an intracellular CO_2 sensor(s) that is associated with anti-inflammatory and immunosuppressive signalling, that is independent of intracellular and extracellular pH and which may account for the above clinical observations. CO_2 can profoundly influence the transcriptional activation of the NF-κB pathway but its transcriptional effects may extend to other as yet uncharacterised pathways. Understanding the molecular

mechanisms of CO_2-dependent intracellular signalling may lead to new therapies where the suppression of immunity or inflammation is clinically desirable.

Acknowledgements

Wild-type and IKKα/β-/- mouse embryonic fibroblasts were a gift from Dr. Inder Verma (Salk Institute, USA). Wild-type mouse embryonic fibroblasts were a gift from. Dr. Alexander Hoffmann (UCSD, USA). Mouse pCR-Flag-IKKalpha expression vector was a gift from Dr. H Nakano.

Figure Legends

Figure 1.

CO_2 exposure causes a rapid, reversible and hypoxia-independent nuclear localisation of IKKα. (A) MEF were treated with control conditions (C), vehicle (V), DMOG (1mM; 0-75 mins) or an atmosphere of 1%O_2 / 5%CO_2 (1hr) without (H) or with (R) 10 minute re-equilibration to ambient conditions (21%O_2 / 0.03%CO_2). **(B)** MEF were exposed to control conditions (C) or 15-21% O_2 / 5% CO_2 without (H) or with (R) re-equilibration to ambient conditions. **(C)** MEF were exposed to 0.03%, 5% or 10% CO_2 (all with 21% O_2) for 1hr without (H) or with (R) re-equilibration to ambient conditions. In all cases, nuclear extracts were prepared and the indicated proteins were identified using western blotting. **(D)** MEF exposed to ambient conditions for 1 hr, 10% CO_2 for 1 hr or 10% CO_2 for 55mins followed by re-equilibration to ambient conditions for 5mins, immunostaining was carried out for IKKα and cells were imaged by con-focal microscopy. (E) PBMCs exposed to 0.03% or 10% CO_2 for 90 mins +/- TNFα (10ng/ml) for final 60 mins. Nuclear extracts were prepared and IKKα was identified using western blotting.

Figure 2.

Elevated CO_2 levels suppress LPS-induced NF-kappaB activity. (A) MEF were exposed to ambient conditions or 10% CO_2 for with or without LPS

treatment (10μg/ml, 1-4hrs). Cytosolic and nuclear extracts were prepared and immunoblotting was carried out using the indicated antibodies. **(B)** MEF transiently transfected with an NF-kappaB-Luc promoter-reporter vector were exposed to ambient conditions or 10% CO_2 for 24hrs with or without LPS treatment (10μg/ml, 24hrs). Cell luciferase levels were analysed by luminometry (n=3 +/- S.E.M, students' t-test)

Figure 3.

Elevated CO_2 attenuates LPS-induced NF-kappaB activity independent of IKKβ. (A) IKKα/β$^{-/-}$ MEF were reconstituted with catalytically active FLAG-tagged IKKα, transfected with an NF-kappaB-Luc reporter plasmid and exposed to ambient conditions or 10% CO_2 for 24hrs with or without LPS treatment (10μg/ml; 24hrs). Reporter activity was analysed by luminometry (n=3 +/- S.E.M, ANOVA). **(B)** IKKα/β-/- MEF were transiently transfected with catalytically active FLAG-tagged IKKα and exposed to ambient conditions or 10% CO_2 (4hrs). Cytosolic and nuclear extracts were prepared and immunoblotting was carried out using the indicated antibodies.

Figure 4.

CO_2-stimulated nuclear IKKα translocation is not inhibited by Acetazolamide, ODQ and Forskolin. (A) Schematic summarising the signaling pathways involved in acute CO_2 sensing in lower species. (relevant references in italics, inhibitors in red). **(B)** MEF were pretreated with Acetazolamide or ODQ for 1hr prior to exposure to ambient conditions or 10% CO_2 (1hr). Acetazolamide, ODQ and Forskollin were added to the media following media change at the time of exposure. Nuclear extracts were prepared and immunoblotting was carried out using the indicated antibodies.

Figure 5.

Elevated CO_2 induces IKKα nuclear translocation when extracellular pH is buffered. (A) MEF were exposed to ambient conditions or 10% CO_2 for 4hrs +/- LPS treatment (10μg/ml, 1-4hrs) with buffered extracellular pH. Media pH was recorded at the start of the experiment and in media taken from the cells at the end (n=3 +/- SEM). **(B)** Cytosolic and **(C)** nuclear extracts were prepared and immunoblotting was carried out using the indicated antibodies.

Figure 6.

Alteration in extracellular or intracellular pH do not promote IKKα nuclear translocation. MEF were exposed to a range of extracellular media-pH conditions (N) neutral (0.03% CO_2 pH 7.54, 10% 7.44) or (A) acidic (0.03% CO_2 pH 7.05, 10% 7.08) under ambient conditions or at 10% CO_2 for 1hr. **(A)**

Cytosolic **(B)** nuclear and **(C)** whole cell extracts were prepared and immunoblotting was carried out using the indicated antibodies. **(D)** Intracellular pH measurements using BCECF fluorescence in MEF exposed to the above conditions (n=3 +/- SEM)

Figure 7. Hypercapnia promotes an anti-inflammatory profile of gene expression. A PCR array of genes known to be involved in the NF-κB signaling cascade was carried out on A549 cells exposed to ambient or 10% CO_2 +/- LT (100ng/ml) for 4hrs. A selection of differentially expressed genes from the array were chosen for validation. **(A)** CCL2, **(B)** ICAM-1, **(C)** TNFα and **(D)** IL-10 message levels were determined by quantitative real-time PCR and expressed as % of LT-induced gene expression at 0.03% CO_2. (n=3+/- SEM, 1-way ANOVA, Tukey post-test)

References

1. Kaelin, W. G., Jr., and P. J. Ratcliffe. 2008. Oxygen sensing by metazoans: the central role of the HIF hydroxylase pathway. *Mol Cell* 30:393-402.
2. Semenza, G. L. 2007. Hypoxia-inducible factor 1 (HIF-1) pathway. *Sci STKE* 2007:cm8.
3. Cummins, E. P., Berra, E, Comerford, K.M., Fitzgerald, K.T., Seeballuck, F, Godson, C, Nielsen, J.E., Moynagh, P, Pouyssegur, J & Taylor, C.T. 2006. Prolyl hydroxylase-1 negatively regulates IkB kinase-beta giving insight into hypoxia-induced NFkB activity. *Proc Natl Acad Sci U S A*.
4. Jones, W. D., P. Cayirlioglu, I. G. Kadow, and L. B. Vosshall. 2007. Two chemosensory receptors together mediate carbon dioxide detection in Drosophila. *Nature* 445:86-90.
5. Hallem, E. A., and P. W. Sternberg. 2008. Acute carbon dioxide avoidance in Caenorhabditis elegans. *Proc Natl Acad Sci U S A* 105:8038-8043.
6. Sun, L., H. Wang, J. Hu, J. Han, H. Matsunami, and M. Luo. 2009. Guanylyl cyclase-D in the olfactory CO2 neurons is activated by bicarbonate. *Proc Natl Acad Sci U S A* 106:2041-2046.
7. Amato, M. B., C. S. Barbas, D. M. Medeiros, R. B. Magaldi, G. P. Schettino, G. Lorenzi-Filho, R. A. Kairalla, D. Deheinzelin, C. Munoz, R. Oliveira, T. Y. Takagaki, and C. R. Carvalho. 1998. Effect of a protective-ventilation strategy on mortality in the acute respiratory distress syndrome. *N Engl J Med* 338:347-354.
8. Laffey, J. G., D. Honan, N. Hopkins, J. M. Hyvelin, J. F. Boylan, and P. McLoughlin. 2004. Hypercapnic acidosis attenuates endotoxin-induced acute lung injury. *Am J Respir Crit Care Med* 169:46-56.
9. Helenius, I. T., T. Krupinski, D. W. Turnbull, Y. Gruenbaum, N. Silverman, E. A. Johnson, P. H. Sporn, J. I. Sznajder, and G. J. Beitel. 2009. Elevated CO2 suppresses specific Drosophila innate immune responses and resistance to bacterial infection. *Proc Natl Acad Sci U S A* 106:18710-18715.
10. Nichol, A. D., D. F. O'Cronin, K. Howell, F. Naughton, S. O'Brien, J. Boylan, C. O'Connor, D. O'Toole, J. G. Laffey, and P. McLoughlin. 2009. Infection-induced lung injury is worsened after renal buffering of hypercapnic acidosis. *Crit Care Med* 37:2953-2961.
11. Hayden, M. S., and S. Ghosh. 2008. Shared principles in NF-kappaB signaling. *Cell* 132:344-362.
12. Takeshita, K., Y. Suzuki, K. Nishio, O. Takeuchi, K. Toda, H. Kudo, N. Miyao, M. Ishii, N. Sato, K. Naoki, T. Aoki, K. Suzuki, R. Hiraoka, and K. Yamaguchi. 2003. Hypercapnic acidosis attenuates endotoxin-induced nuclear factor-[kappa]B activation. *Am J Respir Cell Mol Biol* 29:124-132.

13. Yamamoto, Y., U. N. Verma, S. Prajapati, Y. T. Kwak, and R. B. Gaynor. 2003. Histone H3 phosphorylation by IKK-alpha is critical for cytokine-induced gene expression. *Nature* 423:655-659.
14. Sil, A. K., S. Maeda, Y. Sano, D. R. Roop, and M. Karin. 2004. IkappaB kinase-alpha acts in the epidermis to control skeletal and craniofacial morphogenesis. *Nature* 428:660-664.
15. Anest, V., J. L. Hanson, P. C. Cogswell, K. A. Steinbrecher, B. D. Strahl, and A. S. Baldwin. 2003. A nucleosomal function for IkappaB kinase-alpha in NF-kappaB-dependent gene expression. *Nature* 423:659-663.
16. Hoberg, J. E., A. E. Popko, C. S. Ramsey, and M. W. Mayo. 2006. I{kappa}B Kinase {alpha}-Mediated Derepression of SMRT Potentiates Acetylation of RelA/p65 by p300. *Mol Cell Biol* 26:457-471.
17. Li, Q., G. Estepa, S. Memet, A. Israel, and I. M. Verma. 2000. Complete lack of NF-kappaB activity in IKK1 and IKK2 double-deficient mice: additional defect in neurulation. *Genes Dev* 14:1729-1733.
18. Nakano, H., M. Shindo, S. Sakon, S. Nishinaka, M. Mihara, H. Yagita, and K. Okumura. 1998. Differential regulation of IkappaB kinase alpha and beta by two upstream kinases, NF-kappaB-inducing kinase and mitogen-activated protein kinase/ERK kinase kinase-1. *Proc Natl Acad Sci U S A* 95:3537-3542.
19. Frommer, W. B. Biochemistry. CO2mmon sense. *Science* 327:275-276.
20. Hu, H., A. Boisson-Dernier, M. Israelsson-Nordstrom, M. Bohmer, S. Xue, A. Ries, J. Godoski, J. M. Kuhn, and J. I. Schroeder. Carbonic anhydrases are upstream regulators of CO2-controlled stomatal movements in guard cells. *Nat Cell Biol* 12:87-93; sup pp 81-18.
21. Klengel, T., W. J. Liang, J. Chaloupka, C. Ruoff, K. Schroppel, J. R. Naglik, S. E. Eckert, E. G. Mogensen, K. Haynes, M. F. Tuite, L. R. Levin, J. Buck, and F. A. Muhlschlegel. 2005. Fungal adenylyl cyclase integrates CO2 sensing with cAMP signaling and virulence. *Curr Biol* 15:2021-2026.
22. Wang, N., K. L. Gates, H. Trejo, S. Favoreto, Jr., R. P. Schleimer, J. I. Sznajder, G. J. Beitel, and P. H. Sporn. Elevated CO2 selectively inhibits interleukin-6 and tumor necrosis factor expression and decreases phagocytosis in the macrophage. *Faseb J* 24:2178-2190.
23. Bazzoni, F., N. Tamassia, M. Rossato, and M. A. Cassatella. Understanding the molecular mechanisms of the multifaceted IL-10-mediated anti-inflammatory response: lessons from neutrophils. *Eur J Immunol*.
24. Sharabi, K., A. Hurwitz, A. J. Simon, G. J. Beitel, R. I. Morimoto, G. Rechavi, J. I. Sznajder, and Y. Gruenbaum. 2009. Elevated CO2 levels affect development, motility, and fertility and extend life span in Caenorhabditis elegans. *Proc Natl Acad Sci U S A* 106:4024-4029.
25. Lawrence, T., M. Bebien, G. Y. Liu, V. Nizet, and M. Karin. 2005. IKKalpha limits macrophage NF-kappaB activation and contributes to the resolution of inflammation. *Nature* 434:1138-1143.

26. Hanly, E. J., J. M. Fuentes, A. R. Aurora, S. L. Bachman, A. De Maio, M. R. Marohn, and M. A. Talamini. 2006. Carbon dioxide pneumoperitoneum prevents mortality from sepsis. *Surg Endosc* 20:1482-1487.
27. Nichol, A. D., D. F. O'Cronin, K. Howell, F. Naughton, S. O'Brien, J. Boylan, C. O'Connor, D. O'Toole, J. G. Laffey, and P. McLoughlin. 2009. Infection-induced lung injury is worsened after renal buffering of hypercapnic acidosis. *Crit Care Med*.

Supplementary Figure 1.

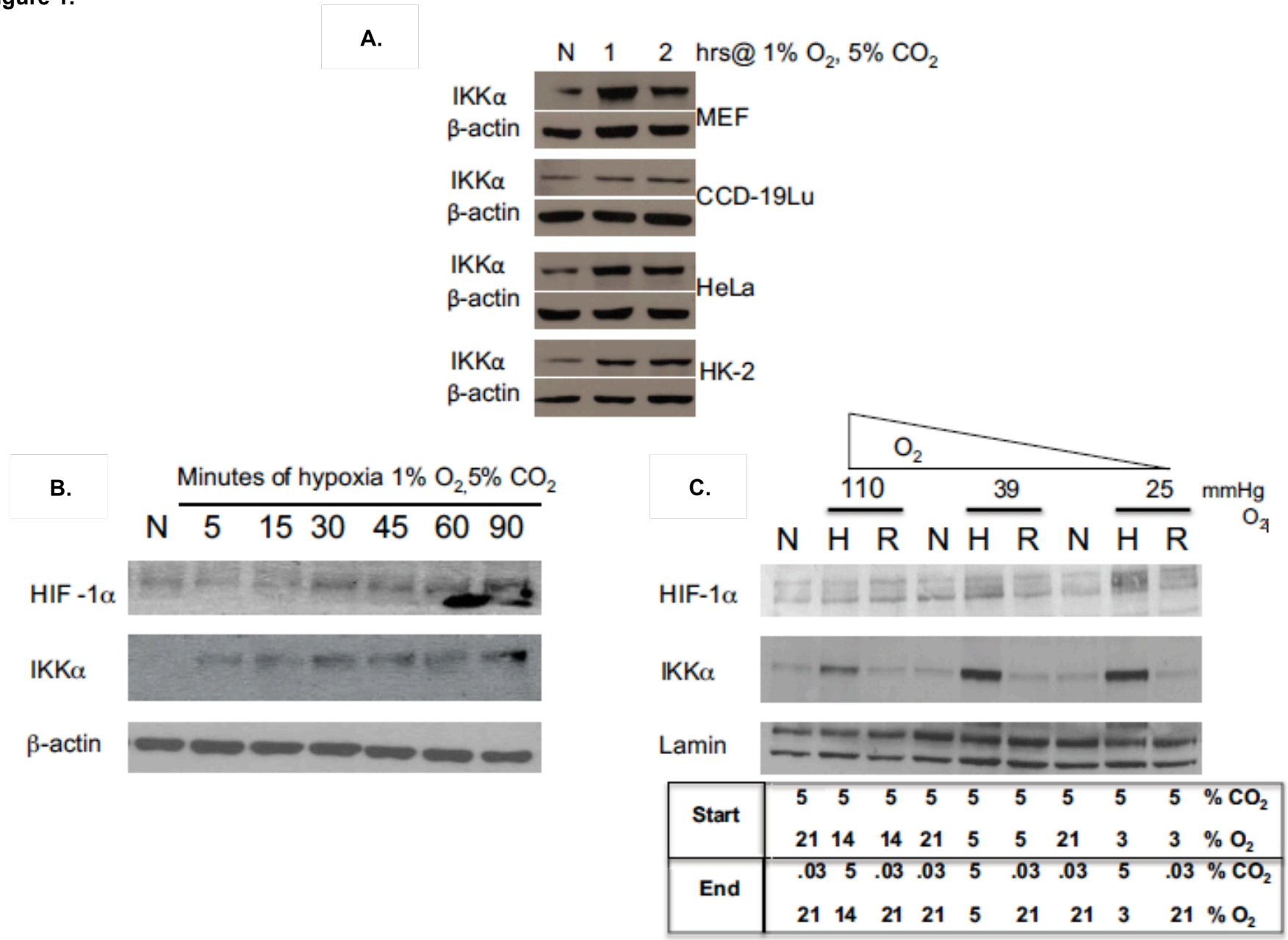

Supplementary Figure 1.

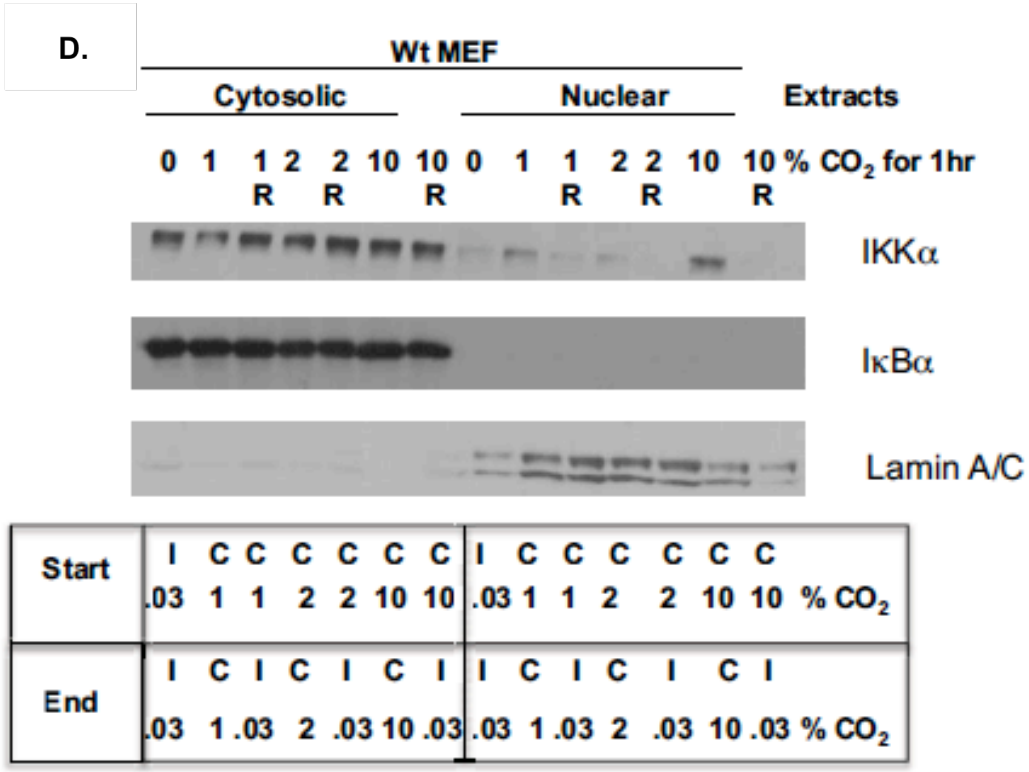

Figure S1. (A) Multiple cell types (MEF, CCD-19Lu, Hela and HK-2) demonstrate accumulation of IKKα in the nuclear fraction following exposure to 1% O_2 / 5% CO_2 (1-2hrs). **(B)** MEF were exposed to 1% O_2 / 5% CO_2 for 0-90 minutes and nuclear translocation of IKKα was determined by western blot. **(C)** MEF were exposed for 1hr to control conditions (C; 21% O_2, 5% CO_2) or 25-110 mmHg O2 / 5%CO2) without (H) or wi th (R) re-equilibration to ambient conditions for 10mins. For A, B and C nuclear extracts were prepared and immunoblotting was carried out using the indicated antibodies. **(D)** MEF were exposed for 1hr to 1, 2 or 10 % C O_2 without or with (R) re-equilibration to ambient conditions for 5mins. Cytosolic and nuclear extracts were prepared and immunoblotting was carried out using the indicated antibodies.

Supplementary Figure 2.

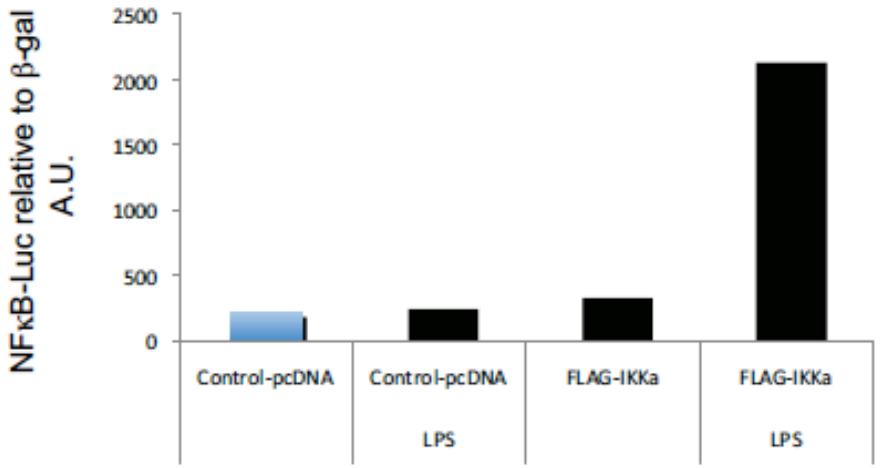

Figure S2. IKKα/β -/- MEF were transiently transfected with an NF-kappaB-Luc promoter-reporter vector or control pcDNA plasmid with or without catalytically active Flag-tagged IKKα and treated with or without LPS (10µg/ml; 24hrs).

Supplementary Figure 3.

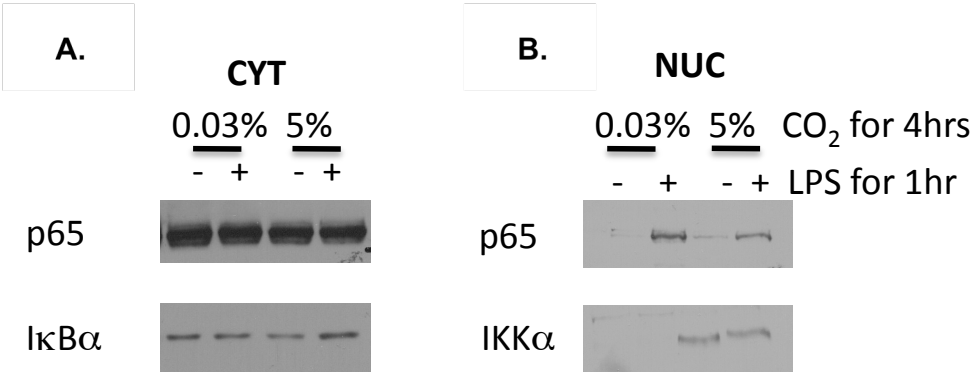

Figure S3. NF-κB signalling is attenuated at 5% CO_2. MEF were exposed ambient or 5% CO_2 for 4hrs +/- LPS (10μg/ml) for the final hour. **(A)** Cytosolic and **(B)** nuclear extracts were prepared and immunoblotting was carried out using the indicated antibodies.

Supplementary Figure 4.

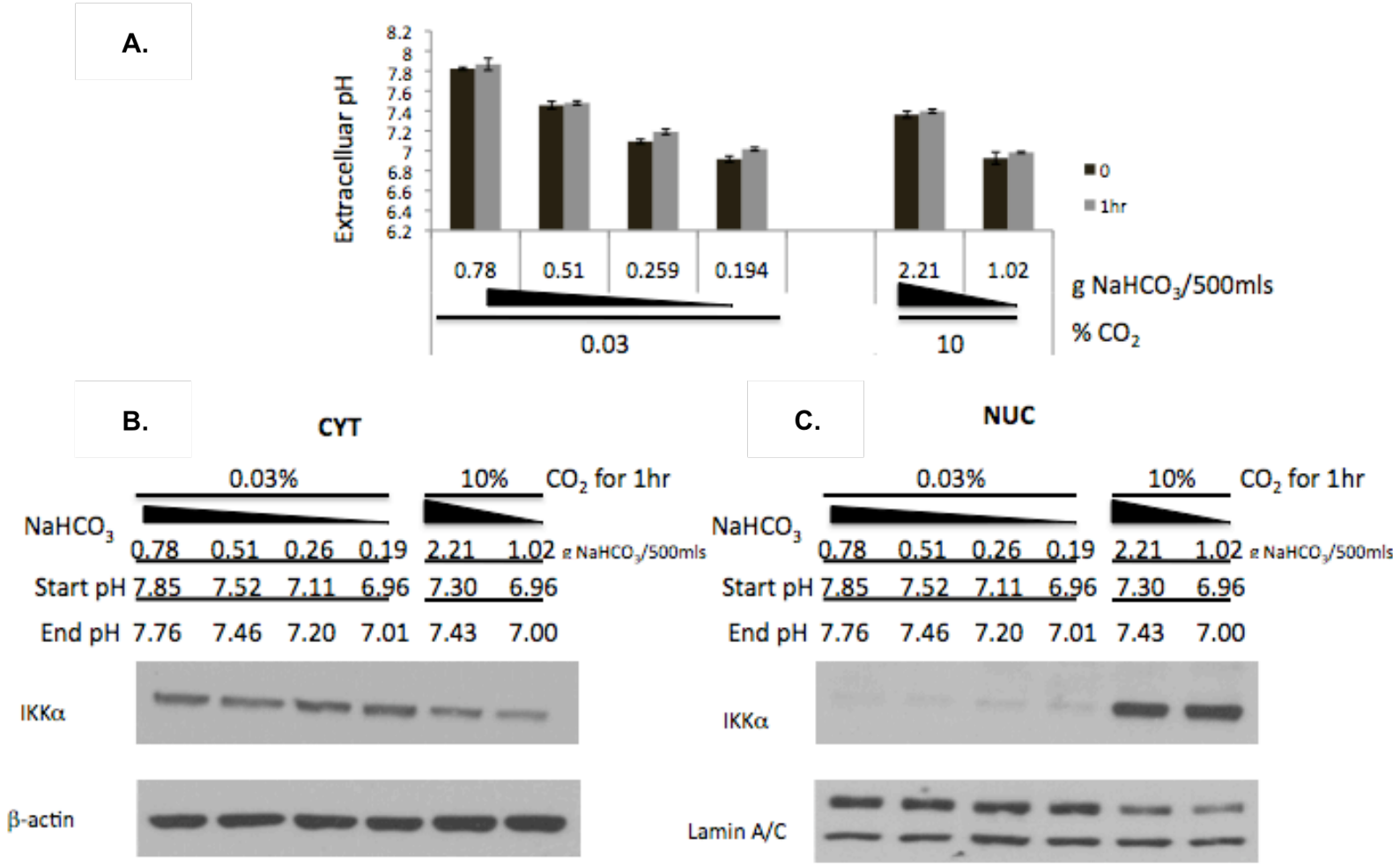

Figure S4. Altered extracellular pH does not promotes IKKα nuclear translocation. (A) MEF were exposed to a range of extracellular media-pH conditions under ambient conditions or at 10% CO_2 for 1hr (n=3+/- SEM). **(B)** Cytosolic and **(C)** nuclear extracts were prepared and immunoblotting was carried out using the indicated antibodies. Results are representative of 3 independent experiments.

Supplementary Figure 5.

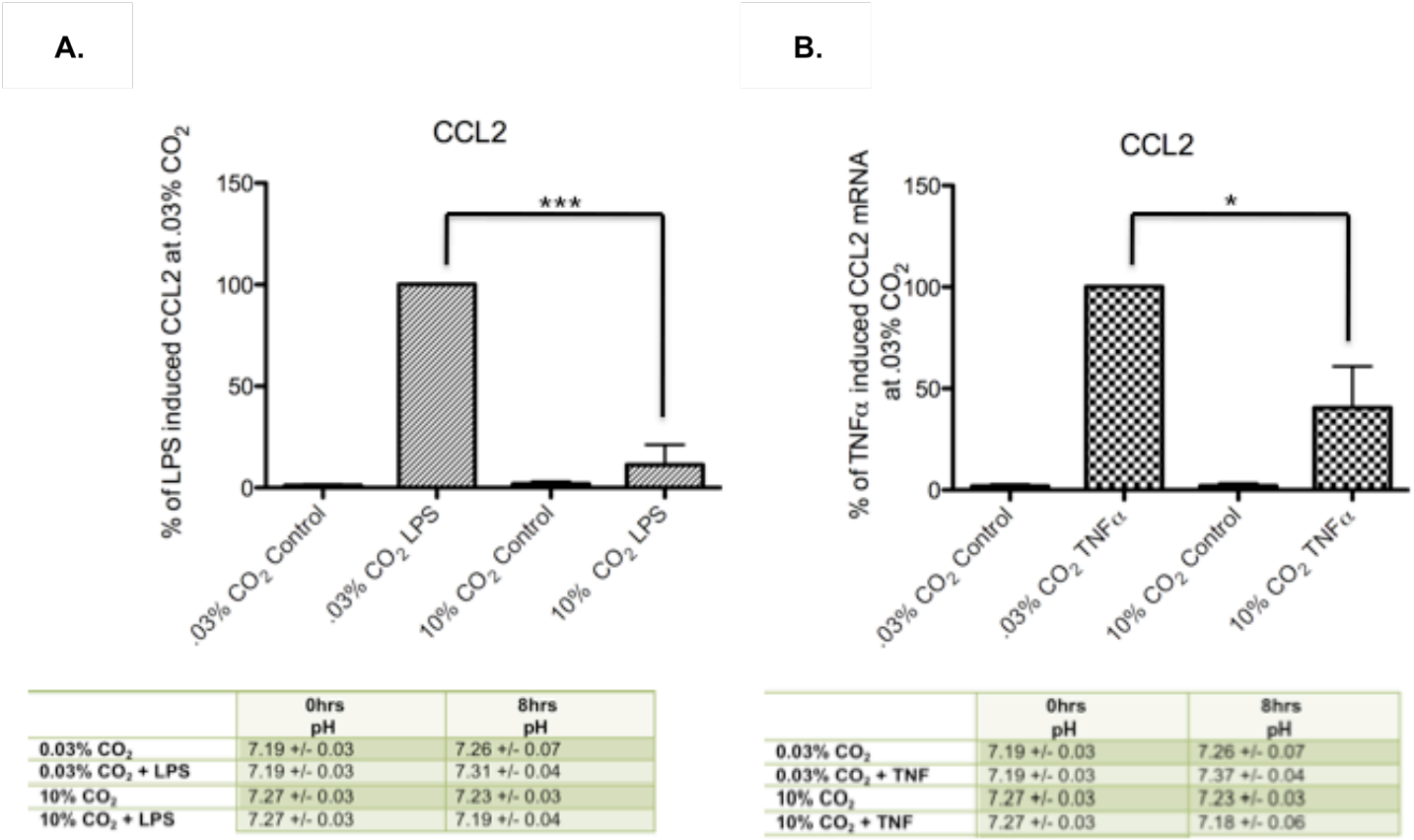

	0hrs pH	8hrs pH
0.03% CO_2	7.19 +/- 0.03	7.26 +/- 0.07
0.03% CO_2 + LPS	7.19 +/- 0.03	7.31 +/- 0.04
10% CO_2	7.27 +/- 0.03	7.23 +/- 0.03
10% CO_2 + LPS	7.27 +/- 0.03	7.19 +/- 0.04

	0hrs pH	8hrs pH
0.03% CO_2	7.19 +/- 0.03	7.26 +/- 0.07
0.03% CO_2 + TNF	7.19 +/- 0.03	7.37 +/- 0.04
10% CO_2	7.27 +/- 0.03	7.23 +/- 0.03
10% CO_2 + TNF	7.27 +/- 0.03	7.18 +/- 0.06

Figure S5. Hypercapnia significantly attenuates ligand-induced CCL2 gene expression. MEF were exposed to ambient conditions or 10% CO_2 for 8hrs with or without LPS (**A**; 10μg/ml, 4hrs) or TNFα (**B;** 10ng/ml, 8 hrs). mRNA was extracted and qRT- PCR performed using CCL2 specific primers. Results are expressed as % of stimulus-induced CCL2 mRNA. n=3 +/- SEM, 1-way ANOVA, Tukey post-test.

Supplementary Figure 6.

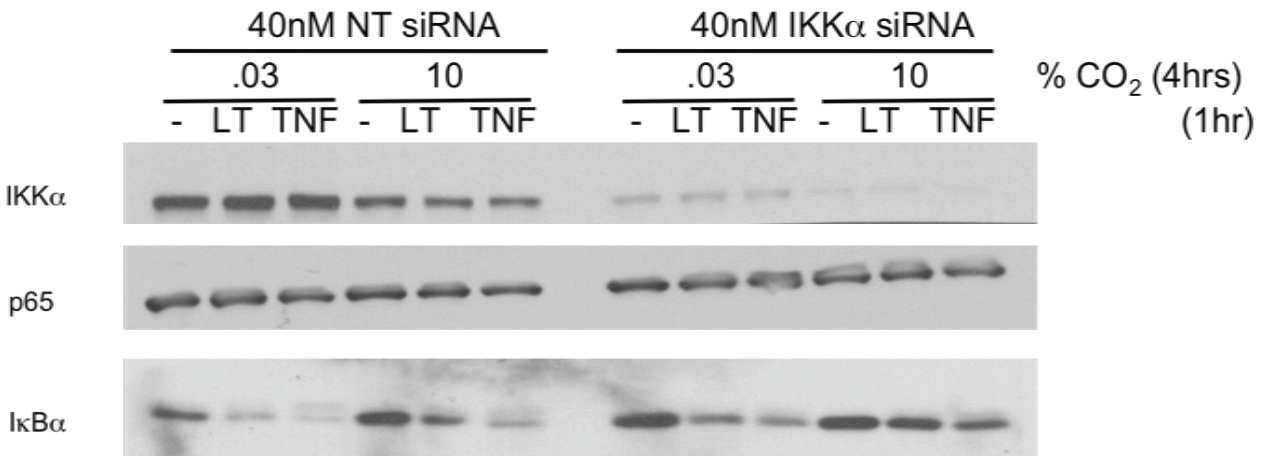

Figure S6. 10% CO_2 maintains cytosolic IκBα in the presence of IKKα siRNA. A549 cells were transfected with 40nM Non-target (NT) or IKKα siRNA for 48 hrs prior to exposure to ambient or 10% CO_2 for 4hrs +/- LT (100ng/ml) or TNFα (10ng/ml) for the final hr of exposure. Cytosolic extracts were prepared and immunoblotted using the indicated antibodies.

Supplementary Figure 7.

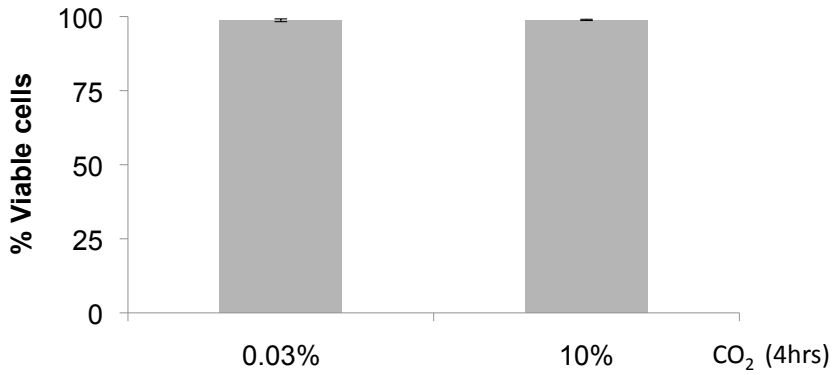

Figure S7. Cell viability is not affected by exposure to 10% CO_2. A549 cells were exposed ambient or 10% CO_2 for 4hrs. Cells were trypsinised and incubated with Tryptan blue dye. Tryptan blue negative cells were scored as viable. Experiments were carried out in duplicate for n=3 experiments. Mean +/- SEM.

Supplementary Table 1.

Raw CT values from NF-kB PCR Array in A549 cells

Gene name	0.03 -	0.03 +	10 -	10 +	% CO_2 4hrs LT (100ng/ml) 4hrs
AKT1	23.97663	23.73151	24.2257	23.32393	
ATF1	21.73064	21.53642	21.76747	21.47381	
BCL10	22.47992	21.82962	21.58967	22.32052	
BCL3	21.89488	21.29234	22.48274	21.65969	
CFB	27.69941	27.36758	27.43692	27.88054	
BIRC2	21.81805	20.43268	20.99767	20.57527	
NOD1	26.16575	26.46038	26.66753	26.53183	
CASP1	29.86272	30.51415	30.81048	30.86117	
CASP8	25.31167	25.16819	24.8434	25.51332	
CCL2	20.88151	18.98169	21.61721	20.90802	
CD40	28.72987	28.49071	28.20054	28.55171	
CFLAR	21.20104	20.56352	21.7611	20.78057	
CHUK	21.98486	21.46662	21.84186	21.83555	
CSF2	29.10461	26.66444	29.00439	28.17647	
SLC44A2	26.79572	26.48336	26.91529	26.74254	
EDARADD	25.77392	25.50117	26.46357	26.6598	
LPAR1	25.51794	24.99782	26.1403	26.45247	
EGR1	31.99064	32.14521	31.08264	31.23978	
ELK1	24.40609	24.28435	24.602	24.54315	
F2R	22.62644	22.78128	22.78475	23.12381	
FADD	24.26713	23.96298	24.25884	24.87444	
FOS	29.18972	29.73708	30.14297	29.64718	
GJA1	21.55672	21.41452	22.82952	21.42483	
HMOX1	19.7543	19.39625	20.09125	20.39915	
HTR2B	26.5617	26.34816	27.80661	27.5473	
ICAM1	27.71808	24.38836	27.18526	25.33878	
IFNA1	30.69918	31.19696	30.14025	29.88741	
IKBKB	24.66358	24.24686	24.40181	24.50679	
IKBKE	26.24004	24.98767	26.70454	25.93726	
IKBKG	25.42929	24.70078	25.17699	25.71442	
IL10	24.80869	24.80972	29.98895	22.97784	
IL1A	27.67809	26.00374	27.54496	27.27643	
IL1B	30.49358	30.23355	31.19569	30.8471	
ILR1	25.41189	25.28645	25.47498	25.51865	
IL6	27.54739	26.48146	27.5045	27.76286	
IL8	25.54832	23.39849	25.30763	23.65343	
IRAK1	24.81669	25.18125	25.9368	25.56042	
IRAK2	22.71979	21.24505	23.9813	22.35627	
JUN	24.53173	24.87353	25.48139	25.14465	
LTA	32.20103	30.92535	33.21802	31.37794	
LTBR	21.61699	21.44431	21.58052	22.09262	
MALT1	22.79718	21.91807	22.89313	22.53633	
MAP3K1	27.62803	26.51098	26.29354	26.27488	
MYD88	24.58316	24.55605	24.73986	24.88276	
NFKB1	20.80291	20.15141	20.44719	20.76312	
NFKB2	28.48248	27.33464	28.34842	27.8731	
NFKBIA	19.93734	18.49733	19.84247	19.50365	
PPM1A	21.77775	22.31793	22.10218	22.63773	
RAF1	22.62455	21.88091	22.23906	23.39162	
REL	24.33031	23.88373	24.73428	24.64647	

RELA	23.10826	22.68484	23.58753	23.22455
RELB	26.402	24.9474	26.77767	25.5765
TRIM13	23.33658	23.2015	24.16085	23.90616
RHOA	19.21121	18.4808	19.58857	19.69799
RIPK1	26.3671	26.23824	26.66044	27.32852
SLC20A1	21.35375	22.16388	21.92192	21.68033
STAT1	20.88024	20.93556	21.71146	21.25892
TBK1	21.92524	21.49418	21.77141	21.92041
TICAM2	25.7278	25.32554	25.56844	24.73442
TLR1	28.80302	28.12619	28.62347	27.69764
TLR2	23.98671	20.29978	22.32283	23.98771
TLR3	28.58579	28.60753	29.22599	30.15971
TLR4	32.34311	33.22715	32.18904	34.39465
TLR6	24.73226	24.21233	24.98659	24.83621
TLR9	24.57783	24.55257	28.43303	23.33098
TMED4	23.42886	22.7097	22.87134	23.23965
TNF	30.83552	28.34008	31.98864	30.69335
TNFAIP3	25.67733	23.70195	26.14933	24.51452
TNFRSF1	26.40092	25.64148	25.82523	24.94752
TNFRSF1	23.26278	22.5953	22.78072	22.24777
TNFRSF1	18.54065	19.28376	18.76489	18.9555
CD27	32.31221	32.93115	32.60917	33.91646
TNFSF10	31.77884	32.54311	33.45213	34.51053
TRADD	23.54925	23.46039	23.31862	23.65735
TICAM1	26.1564	26.14259	25.15703	25.54546
B2M	19.17804	18.31631	18.77141	19.00088
PTGS2	22.24598	21.43064	21.77837	21.17759